

03.1

Heat transfer enhancement in an inclined boomerang groove on a heated channel wall with the end portion oriented along the flow

© S.A. Isaev^{1,2}, D.V. Nikushchenko¹, I.A. Popov³, A.A. Mironov³, A.A. Klyus²,
A.G. Sudakov²

¹ State Marine Technical University, St. Petersburg, Russia

² Novikov St. Petersburg State University of Civil Aviation, St. Petersburg, Russia

³ Tupolev Kazan National Research Technical University (KAI), Kazan, Tatarstan, Russia

E-mail: isaev3612@yandex.ru

Received May 6, 2024

Revised June 25, 2024

Accepted June 25, 2024

An anomalous intensification of the separated turbulent flow and heat transfer in inclined straight grooves on the channel wall and plate is characterized by weakening of vortex structures and suppression of heat transfer in the end part of the groove. It has been established that the fracture of the groove end part oriented along the flow in the channel with its optimal relative length leads to penetration of an intense swirling flow into the groove end zone and intensifies heat transfer in it. Relative heat transfer from the surface inside such a boomerangtype groove increases by 1.2 times compared to that in the straight inclined groove.

Keywords: separated flow, narrow channel, inclined boomerang groove, intensification, numerical modeling.

DOI: 10.61011/0000000000

A variety of surface vortex generators in the dimpled technologies is shown in review [1]. Dimples are proposed as antipodes of protrusions as elements of the structured surface discrete roughness, which are characterized by radically lower hydraulic losses. The desire to reduce hydraulic losses of structured surfaces led to profiling the dimples, primarily to smoothing their edges, and also to making the dimple shapes asymmetrical and connecting them in pairs, for instance, in the form of *V*-shaped configurations. First of all, let us point to teardrop stream-wise and counter-stream-wise dimples often found in literature (see, e.g. [2]) and circular asymmetric dimples with stream-wise and counter-stream-wise shifting of the deepest bottom point [3]. Interest in generating intense vortex structures in the dimples initiated development of *V*-shaped dimples [4]. Widely varying symmetrical and asymmetrical dimples under consideration are joined together by one common inherent property: they are quite compact and have moderate extensions. It is interesting to emphasize that, when ordered systems of such compact roughness are flown around, separation zones get formed inside them, and heat transfer gets significantly suppressed [5].

During turbulent flowing around the inclined grooves that are elongated oval-trench dimples, the effect of heat transfer intensification inside the groove, which is abnormal for separated flows, was detected in a single-row package on the heated narrow channel wall in the stabilized hydrodynamic section [6]. The minimum negative friction and maximum Nusselt number in the zone of return currents are many times (5–7 times for a dense package) greater in absolute value than friction and Nusselt number in a plane-parallel channel. On the structured channel wall with inclined

grooves, a significant enhancement of heat transfer occurs in the zones of separated flow inside the grooves. The mechanism of abnormal intensification of the separated flow and heat transfer in the inclined grooves is associated with the emergence of extraordinary pressure differences concentrated in narrow inlet sections [7,8], the areas of negative pressure in the inlet spherical segments being caused by formation of tornado-like structures. Analysis of the calculated and measured distribution of the relative Nusselt number in the central crosssection of a single inclined groove on the plane plate [9] showed its twofold increase over that in the case of a plane plate in the inlet part and a rather sharp decrease in the end part. The heat transfer suppression is also observed in the groove end parts in a single-row package on the channel wall [6]. The reason for the sharp decrease in the relative heat transfer is associated with a decrease in the end-part vortex flow intensity caused by early exit of the spiral vortex from the inclined groove.

In this work we propose to profile a boomerang groove by changing its trajectory and orienting streamwise its end part (Fig. 1). As in [10,11], a single groove with the inlet part inclined at 45° is located on the channel wall. Input part relative length ξ varies from zero to unit, i.e. the streamwise groove gets transformed into an inclined straight groove. Channel height $H = 0.05$ m is taken as a characteristic size. The channel dimensionless width is 2, while length is 12. The groove consists of two semi-spherical dimples attached to each other by a trench insert; its width is 0.6, depth is 0.15, and total length is 3. Its inlet part with variable relative length ξ is inclined at angle 45°, while the end part is directed streamwise. The edge rounding

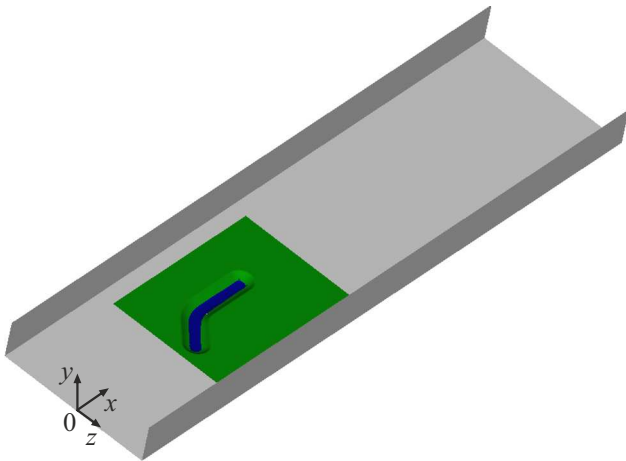


Figure 1. A narrow channel with a groove on its heated wall; Cartesian frame of reference x , y , z with the origin in the middle of the channel inlet crosssection is shown. $\xi = 0.4$. The upper channel wall is removed.

radius is 0.02. The groove is located in the middle of the channel at the distance of 6 from the inlet crosssection. The Reynolds number determined from the uniform flow velocity at the inlet and channel height is set to $1.65 \cdot 10^4$. The boundary layer thickness at the inlet of channel working part is about 0.1. On the wall, dimensionless values of the x -component of friction stress f and pressure P are determined based on the characteristic velocity chosen to be the inlet uniform flow velocity. The degree of turbulence in the inlet crosssection is assumed to be 0.5%; the turbulence scale is taken equal to characteristic size H . The no-slip condition is specified on the walls, while on the outlet boundary the conditions for continuation of solution are specified. At the channel inlet, the air flow is isothermal with temperature $T_{ref} = 293$ K. The lower flow-exposed groove-containing wall of the channel is heated, the supplied constant heat flux q being reduced to the dimensionless form via $q^* = q/[\lambda \cdot \text{Pr} \cdot \text{Re} \cdot T_{ref}/H]$ and assumed to be $3.4 \cdot 10^{-5}$. Here λ is the air thermal conductivity, $\text{Pr} = 0.7$. Side walls of the channel are adiabatic; the upper wall is isothermal with temperature T_{ref} taken as the non-dimensionalization scale. Temperature T at the channel outlet meets soft boundary conditions. Nusselt number Nu is determined from the temperature gradient on the wall and difference between the wall temperature and average mass temperature in the relevant channel crosssection.

Convective heat transfer in the low-velocity turbulent flow in a channel with an inclined boomerang groove located on the heated wall will be calculated based on the Reynolds-averaged Navier–Stokes equations for incompressible fluid closed by using the Menter’s shear stress transfer model, and on energy [6–9]. The set of initial stationary equations in the linearized form will be solved using multi-block computing technologies and partially intersecting different-scale structured grids [1–4]. The multi-block computing grid

consisting of four fragmentary grids contains about $4 \cdot 10^6$ cells. The near-wall pitch is 10^{-5} . The numerical simulation procedure is the same as in [11].

Fig. 2 presents the results of comparing the distributions of relative friction f/f_{pl} and static pressure P non-dimensionalized by the double velocity head in the fixed reference frame s , t in the median longitudinal and inlet transverse crosssections of the groove with varying from zero to unit the ratio of the inclined part length to total groove length ξ . Characteristic parameters with index pl are taken at the plane-parallel channel points corresponding to projections of the grooved curved wall of the channel. The inlet groove crosssection is the crosssection of the joint between spherical segment and trench insert.

The dynamics of variations in relative friction with increasing ξ is important for analyzing intensification of the separated flow and heat transfer in a boomerang groove. As the length of the groove inlet inclined part increases, the return current intensity in the median crosssection increases (Fig. 2, *a*) and quite quickly (at $\xi = 0.4$) reaches the f/f_{pl} minimum of about -1.8 which is many times higher in modulus than $(f/f_{pl})_{\min}$ for the streamwise groove. It is interesting to note that the $f/f_{pl}(s)$ distributions in the inlet part at $\xi > 0.3$ are practically coincident, i.e. the headpart return flow gets stabilized. It is important to emphasize that, when the inclined part relative length is $\xi = 0.3$, the f/f_{pl} maximum is reached in the streamwise end part of the groove and exceeds the planewall relative friction by 30%. As ξ increases, the f/f_{pl} maximum decreases to approximately 0.25 at $\xi = 0.6$; therewith, local maximum $f/f_{pl} = 0.6$ emerges in the middle of the groove. As ξ continues increasing, this maximum shifts away from the center with a certain increase (0.7 at $\xi = 0.7$) and then decreases in magnitude (0.5 at $\xi = 0.8$ and 0.4 at $\xi = 1$). At the end of the groove there is a narrow separation zone with the minimum value $(f/f_{pl})_{\min} = -0.45$ at $\xi = 0.3$. As ξ continues growing, this minimum first approaches zero and even becomes positive at $\xi = 0.6$. Further increase in ξ is accompanied by expansion of the separation zone at the end of the groove, but its intensity for the straight groove decreases. When ξ rises above 0.3, relative friction and pressure distributions in the characteristic transverse crosssection of the groove inlet part become almost fully coinciding. Value of $(f/f_{pl})_{\min}$ reaches -2 closer to the windward slope, while the pressure drop reaches 0.21 with $P_{\min} = -0.08$.

The Table presents the values of thermal efficiency $\text{Nu}_m/\text{Nu}_{m,pl}$ of the curved surface confined by the groove contour, relative hydraulic resistance ξ/ξ_{pl} of the channel part between the inlet and end groove crosssections, and its thermal-hydraulic efficiency. At the optimal relative length $\xi = 0.4$, $\text{Nu}_m/\text{Nu}_{m,pl}$ radically exceeds thermal efficiency of the streamwise straight groove and is significantly higher (1.2 times) than in the case of the inclined straight groove. It is important to note that, therewith, the increase in relative hydraulic losses appeared to be lower than that in thermal efficiency (1.2 against 1.29). What is also interesting is that

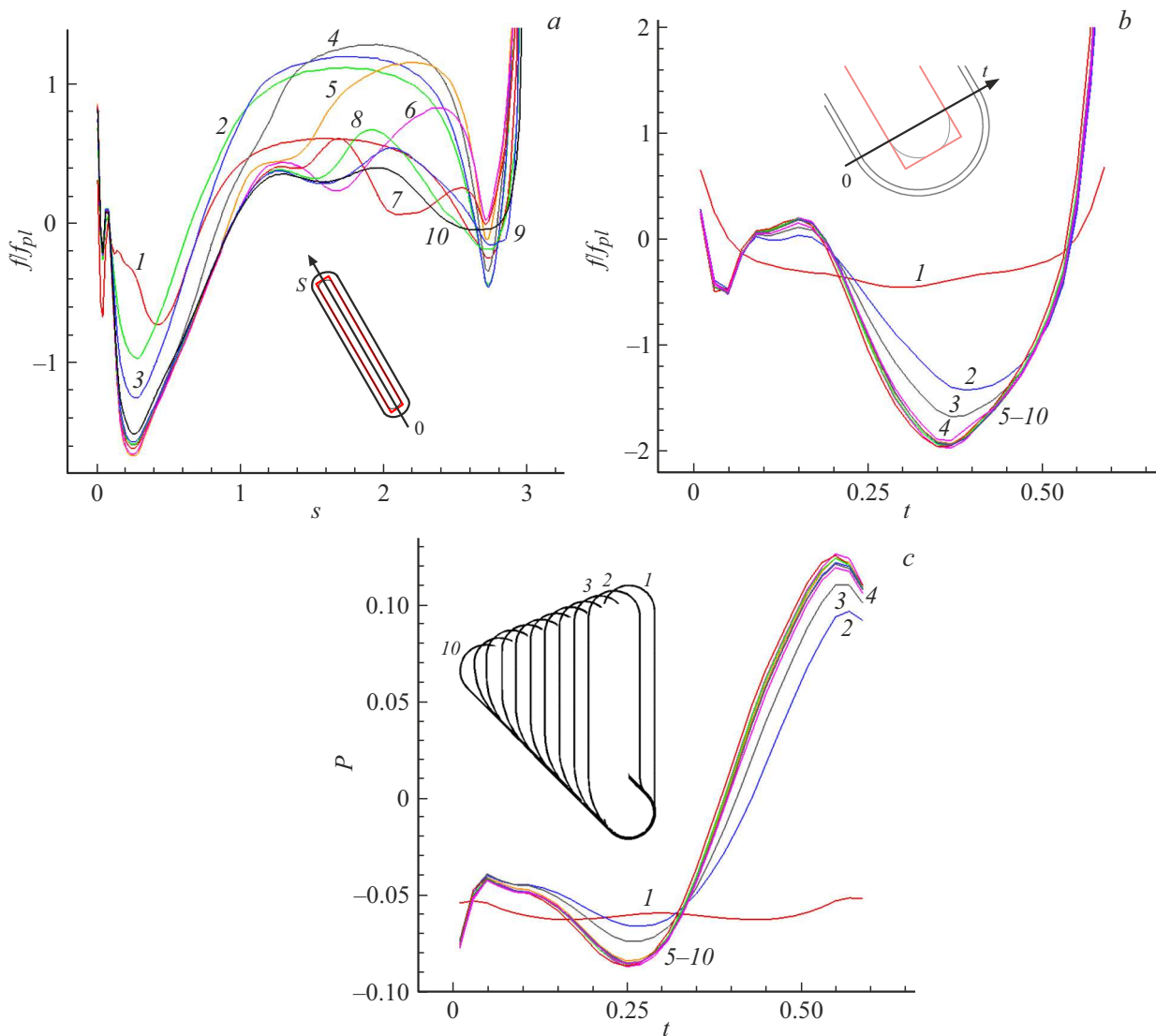


Figure 2. Distributions of relative friction f/f_{pl} (a, b) and pressure P (c) in the central (a) and characteristic inlet (b, c) crosssections of the groove surface for various ratios of the inclined part length to the groove length: $\xi = 0$ (1), 0.15 (2), 0.2 (3), 0.3 (4), 0.4 (5), 0.5 (6), 0.6 (7), 0.7 (8), 0.8 (9) and 1 (10). The insets to panels a, b show orientation of axes of the fixed reference frame s, t ; the inset to panel c shows the evolution of the boomerang groove contours for different ξ .

The influence of the ratio between the inclined section length and total boomerang groove length on the relative heat transfer from the area confined by the groove spot contour, and also on hydraulic losses in the channel part between the groove inlet and end cross-sections and thermal-hydraulic efficiency of the groove surface

ξ	$Nu_m/Nu_{m\,pl}$	ξ/ξ_{pl}	$(Nu_m/Nu_{m\,pl})/(\xi/\xi_{pl})^{1/3}$
0	0.96	1.07	0.94
0.4	1.29	1.20	1.215
1	1.07	1.16	1.015

thermal-hydraulic efficiency of straight grooves is low, while at the optimal boomerang groove length it is quite high and equals 1.215.

The source of high thermal and thermohydraulic efficiency of the groove with $\xi = 0.4$ is made evident in Fig. 3. In the case of a straight groove, a spiral vortex organized inside the groove leaves it prior to reaching the end. The groove trajectory bend at the optimal inclined part length enables retaining the swirling flow in the groove right up to its end. Thus, when $\xi = 0.4$, the maximum heat removal from the groove inner surface is obtained (see the Table), and the maximum endpart friction also significantly exceeds the friction on the plane-parallel channel wall.

As a result, the fracture of the streamwise groove end section in the channel with the optimal relative length was shown to promote penetration of a swirled flow into the groove end part and intensify heat transfer in it. A 1.2 times increase in relative heat transfer from the boomerang

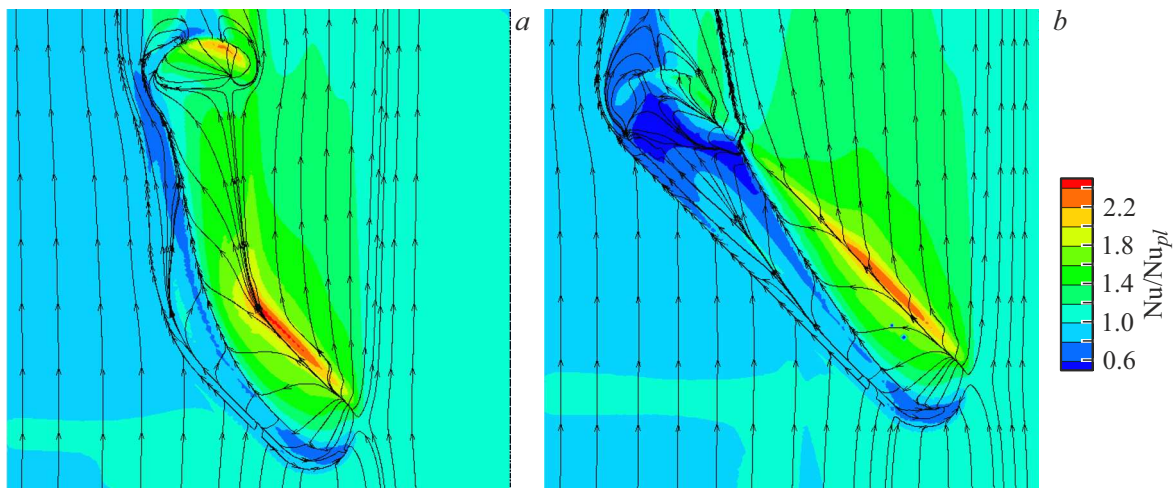


Figure 3. Comparison of fields of relative Nusselt numbers Nu/Nu_{pl} with superimposed patterns of spreading on the heated channel surface with inclined boomerang grooves with a trajectory bend for $\xi = 0.4$ (a) and constant slope (b).

groove inner surface over that in the straight inclined groove is observed.

Funding

The study was supported by the Russian Science Foundation (projects 22-19-00056 (testing) and 23-19-00083 (calculations)).

Conflict of interests

The authors declare that they have no conflict of interests.

References

- [1] S. Rashidi, F. Hormozi, B. Sunden, O. Mahian, *Appl. Energy*, **259**, 1491 (2019). DOI: 10.1016/j.apenergy.2019.04.168
- [2] Y. Rao, B. Li, Y. Feng, *Exp. Therm. Fluid Sci.*, **61**, 201 (2015). DOI: 10.1016/j.expthermflusci.2014.10.030
- [3] Y. Chen, Y.T. Chew, B.C. Khoo, *Int. J. Heat Mass Transfer*, **55**, 8100 (2012). DOI: 10.1016/j.ijheatmasstransfer.2012.08.043
- [4] C.N. Jordan, L.M. Wright, *J. Turbomach.*, **135**, 011028 (2013). DOI: 10.1115/1.4006422
- [5] P. Zhang, Y. Rao, P.M. Ligrani, *Int. J. Therm. Sci.*, **177**, 107581 (2022). DOI: 10.1016/j.ijthermalsci.2022.107581
- [6] S.A. Isaev, M.S. Gritckevich, A.I. Leontiev, O.O. Milman, D.V. Nikushchenko, *Int. J. Heat Mass Transfer*, **145**, 118737 (2019). DOI: 10.1016/j.ijheatmasstransfer.2019.118737
- [7] S.A. Isaev, *Fluid Dyn.*, **57** (5), 558 (2022). DOI: 10.1134/S0015462822050081
- [8] S.A. Isaev, S.V. Guvernyuk, D.V. Nikushchenko, A.G. Sudakov, A.A. Sinyavin, E.B. Dubko, *Tech. Phys. Lett.*, **49** (8), 33 (2023). DOI: 10.61011/TPL.2023.08.56684.19560.
- [9] S.A. Isaev, S.Z. Sapozhnikov, D.V. Nikushchenko, V.Yu. Mityakov, V.V. Seroshtanov, E.B. Dubko, *Fluid Dyn.*, **59** (1), 45 (2024). DOI: 10.1134/S0015462823602310
- [10] M.A. Zubin, A.F. Zubkov, *Fluid Dyn.*, **57** (1), 77 (2022). DOI: 10.1134/S0015462822010128.

- [11] S.A. Isaev, A.G. Sudakov, D.V. Nikushchenko, V.B. Kharchenko, L.P. Iunakov, *Fluid Dyn.*, **58** (6), 1004 (2023). DOI: 10.1134/S0015462823601304

Translated by EgoTranslating